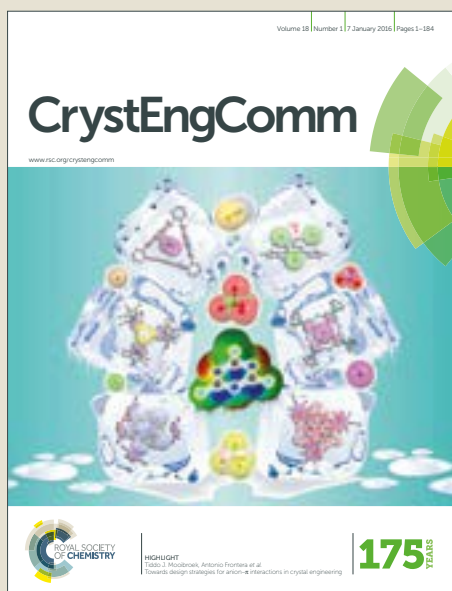


CrystEngComm

Accepted Manuscript



This article can be cited before page numbers have been issued, to do this please use: I. Hisaki, E. N. Q. Affendy and N. Tohnai, *CrystEngComm*, 2017, DOI: 10.1039/C7CE00183E.



This is an Accepted Manuscript, which has been through the Royal Society of Chemistry peer review process and has been accepted for publication.

Accepted Manuscripts are published online shortly after acceptance, before technical editing, formatting and proof reading. Using this free service, authors can make their results available to the community, in citable form, before we publish the edited article. We will replace this Accepted Manuscript with the edited and formatted Advance Article as soon as it is available.

You can find more information about Accepted Manuscripts in the [author guidelines](#).

Please note that technical editing may introduce minor changes to the text and/or graphics, which may alter content. The journal's standard [Terms & Conditions](#) and the ethical guidelines, outlined in our [author and reviewer resource centre](#), still apply. In no event shall the Royal Society of Chemistry be held responsible for any errors or omissions in this Accepted Manuscript or any consequences arising from the use of any information it contains.

Precise Elucidations on Stacking Manners of Hydrogen-Bonded Two-Dimensional Organic Frameworks Composed of X-Shaped π -Conjugated Systems

Ichiro Hisaki,* Nur Qadya Emilya Binti Affendy and Norimitsu Tohnai

Received 00th January 20xx,
Accepted 00th January 20xx

DOI: 10.1039/x0xx00000x

www.rsc.org/

Two-dimensional covalent organic frameworks (2D-COF) composed of π -conjugated components are promising functional materials. In general, however, 2D-COFs exhibit low crystallinity, preventing precise structural characterization. On the other hand, non-covalent organic frameworks (nCOFs) are often obtained as a single crystals due to highly reversible bond formation, and therefore, are possible to complement structural evaluation of 2D-COFs. In this study, three X-shaped tetracarboxylic acid derivatives with benzene, tetrathiofruvallene (TTF), and pyrazinoquinoxaline cores (**X-Ph**, **X-TTF** and **X-PyQ**, respectively) were revealed to form isostructural, hydrogen-bonded rhombic network (RhomNet) sheets, which subsequently stacked without interpenetration to give low density frameworks with one-dimensional (1-D) inclusion channel. RhomNet structures and their stacking manners were fully revealed based on single crystal X-ray analysis. Consequently, we revealed that the RhomNet sheets of **X-Ph**, **X-TTF** and **X-PyQ** stack in different ways depending on conformation of the peripheral phenylene groups, molecular symmetry and interlayer interactions, in spite of the same network topology in the RhomNet sheets. The precise characterization of the present RhomNet crystals can provide a new structural insight of porous 2D-COFs.

Introduction

Organic porous materials have intensively explored from viewpoints of selective gas separation and storage, sensors and catalysts.¹ Particularly, porous materials formed by stacking of two-dimensionally (2D) networked π -conjugated organic components have attracted much attention due to potential application for photoelectronic devices. One of the promising systems is 2D covalent organic frameworks (2D-COFs).² To date, a number of excellent 2D-COFs have been prepared with various π -conjugated organic building blocks and their optical and electronic properties have been reported.^{2,3}

Structural characterization of 2D-COFs is, however, conducted by powder X-ray diffraction (PXRD) analysis combined with other spectroscopic methods, such as solid state NMR, to estimate how porous 2D sheet are stacked to form layered structures (e.g. staggered, inclined, serrated, eclipsed or other manners). For example, O. Yaghi reported that COF-1 has a graphite-like staggered stacking manner.⁴ Yan reported PI-COFs with a serrated-type stacking manner.⁵ A stacking manner was also precisely investigated by theoretical

approaches.⁶ However, in most cases of 2D-COFs, it is concluded that 2D-COF sheets are laminated with an eclipsed manner.

In connection with crystallinity of 2D-COFs, F. Auras, T. Bein and co-workers recently developed a new synthetic concept to allow highly crystalline 2D-COFs.⁷ Namely, 2D networked sheets composed of propeller-shaped molecular building blocks can suppress irregular offset stacking of the sheets to yield fully eclipsed structures with high crystallinity.⁷ However, it still remains difficult in general to obtain precise structural information, particularly subtle slipping of the stacked layers and conformation of flexible parts.

In this context, non-covalent organic framework (nCOF),⁸ including hydrogen-bonded organic frameworks (HOFs),^{9a} supramolecular organic frameworks (SOFs),^{9b} and porous organic salts (POSSs),^{9c} is a convenient model system because facile processing such as recrystallization can provide highly crystalline precipitates suitable for precise structural characterization by single crystal X-ray diffraction analysis. Indeed, detailed structures of a number of 2D-nCOFs have been reported so far.¹⁰

Recently, we also demonstrated that a series of C_3 -symmetric π -conjugated systems possessing six carboxy phenyl groups (**Tp**, **T12**, **T18** and **Ex**) crystallized into 2D-nCOF,¹¹ in which a multi-porous hexagonal network (HexNet) is formed and stacked without interpenetration to yield layered assemblies (Fig. 1a,b). It is remarkable that the HexNet layers does not stack with an eclipsed manner but in an inverted manner with more complex overlapping of the frameworks,

^a Department of Material and Life Science, Graduate School of Engineering, Osaka University, 2-1 Yamadaoka, Suita, Osaka 565-0871, Japan. E-mail: hisaki@mls.eng.osaka-u.ac.jp

[†] Electronic Supplementary Information (ESI) available: Crystallographic information files (CIFs), TG analysis curves, ¹H and ¹³C NMR spectra of the newly synthesized compounds. See DOI: 10.1039/x0xx00000x

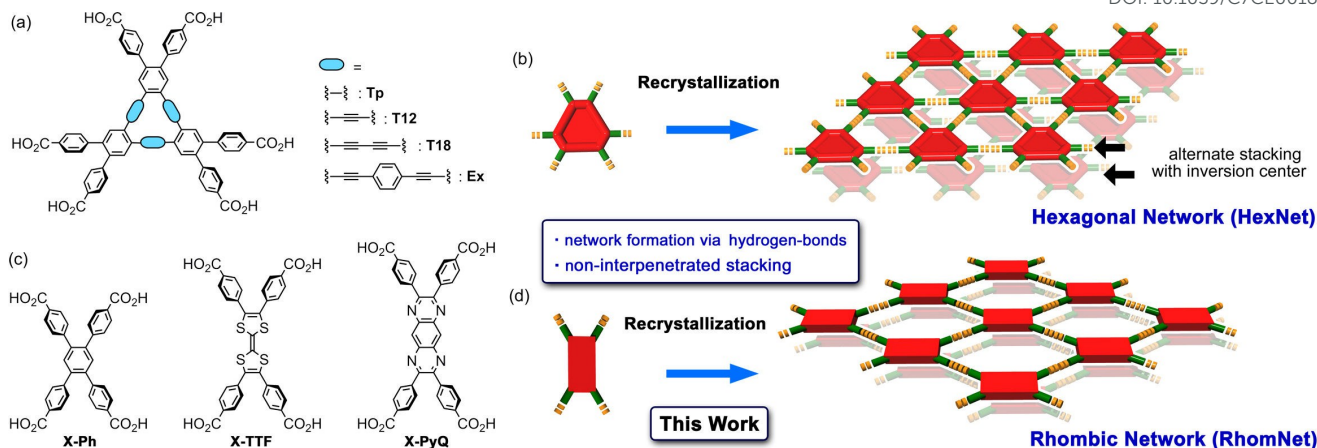


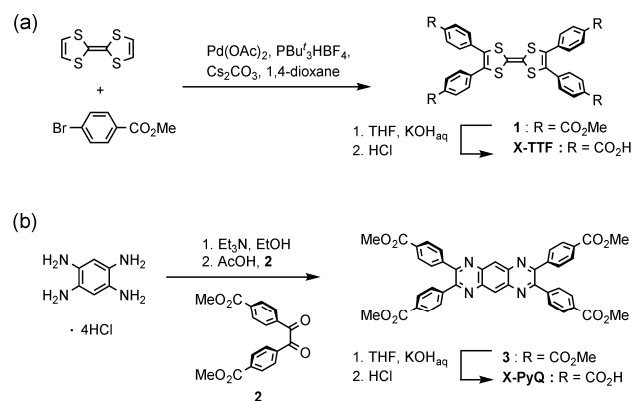
Fig. 1 Construction of hydrogen-bonded organic frameworks with two-dimensional network motifs. (a) C_3 -symmetric and (c) X-shaped molecules with 4-carboxyphenyl groups. Schematic representation for formation of a layered assembly of (b) hexagonal and (d) rhombic networks (HexNets and RhomNets, respectively) composed of the corresponding C_3 -symmetric and X-shaped building blocks. In the case of (b), HexNets sheets alternately stacked related with inversion operation, resulting no eclipse stacking but more complex stacking manner as we previously observed. In the case of this work with X-shaped molecules, on the other hand, even when sheets stack with inversion center, the resulting layered assemblies can form nearly eclipsed stacking manner.

depending on C_3 -symmetric cores applied. These observation prompt us to explore a stacking manner of layers in other types of 2D-nCOFs.

In this manuscript, we report that layered assemblies of isostructural, hydrogen-bonded, rhombic network (RhomNet) were constructed by using a series of X-shaped molecules with two sets of neighbouring 4-carboxyphenyl groups; namely, benzene derivative **X-Ph**, electron donative tetrathiofulvalene (TTF) derivative **X-TTF**, and electron acceptable pyrazinoquinoxaline derivative **X-PyQ** (Fig. 1c,d).

Although MOFs¹² and COFs¹³ based on X-shaped molecules have been reported so far, this is the first demonstration that isostructural RhomNets were formed from a series of X-shaped tetracarboxylic acids with different π -conjugated cores through hydrogen bonds between carboxyl groups. Moreover, in the case of X-shaped molecules, even when sheets stack with inversion center, the resulting layered assemblies can yield a much simpler stacking manner compared with the previously reported HexNets sheets composed of C_3 -symmetric molecules due to higher symmetric molecular shape.

Indeed, single crystal X-ray diffraction analysis showed that RhomNet sheets in the all systems were stacked without interpenetration to give 2D-nCOFs possessing 1D inclusion channels. We revealed that stacking manner of the sheets, which looks quite similar at a glance, is different from each other depending on conformation of the peripheral phenylene groups as well as molecular symmetry. Thus, we believe that precise characterization of the present 2D-nCOFs with a RhomNet structure can provide a deeper insight into structural consideration of porous 2D-COFs.



Scheme 1 Synthesis of X-shaped building blocks, (a) **X-TTF** and (b) **X-PyQ**.

Results and discussion

Preparation of building blocks and 2D-nCOFs. Compound **X-Ph** was commercially available. **X-TTF** was synthesized through a palladium catalyzed cross coupling between TTF and methyl 4-bromobenzoate followed by hydrolysis (Scheme 1a), according to literature.¹⁴ **X-PyQ** was synthesized by condensation of 1,2,4,5-tetraaminobenzene with dimethyl 4,4'-oxalylidibenzate followed by hydrolysis (Scheme 1b). Each of **X-Ph**, **X-TTF**, and **X-PyQ** was recrystallized from a mixed solvent of dimethylformamide (DMF) and *o*-dichlorobenzene (*o*DCB) with a ratio of 1:1 at ranging from 70 °C to 100 °C, yielding single crystals of RhomNet frameworks (**X-Ph-1**, **X-TTF-1**, and **X-PyQ-1**, respectively) suitable for X-ray crystallographic analysis. Crystal structures of **X-Ph-1**, **X-TTF-1**, and **X-PyQ-1** are shown in Figs. 2-4. ‡

Crystal structures. Crystal structure of **X-Ph-1** belongs to space group *Pbcn* (Fig. 2). The structure consists of a conformer of **X-Ph** with a C_2 symmetry. Peripheral carboxy groups of **X-Ph** form a typical self-complementary dimer through directional hydrogen bonds, resulting a 2D-networked Rhombic sheet (RhomNet). The sheet has a void with a dimension of ca. $12.5 \text{ \AA} \times 24.8 \text{ \AA}$ and is stacked in a serrated ABAB manner with an average interlayer distance of 4.6 \AA . Twisted angle of the phenylene groups and the benzene core ranges $51.1\text{--}52.7^\circ$. Main interlayer interactions are face-to-edge (CH/π) contacts between the peripheral carboxyphenyl groups, for example, those of the groups I and II shown in Fig 2c, and there is no significant interaction between the central

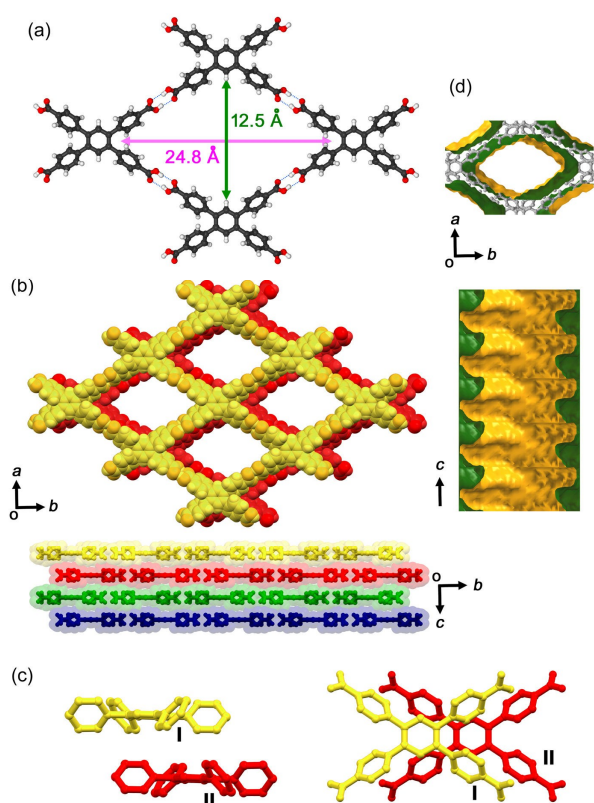


Fig. 2 Crystal structures of RhomNets **X-Ph-1** (a) hydrogen-bonded network motif composed of four molecules. (b) Selected four layers of porous rhombic sheets viewed from above (top) and side (bottom). (c) Orientation of two adjacent molecules, where the carboxyphenyl groups I and II are arranged in face-to-edge manner. The carboxy groups are omitted for clarity in (c)-(left). (d) Visualized inclusion channel surface. Solvent molecules (i.e. *o*DCB) are included in void spaces, although those are not shown in Figures due to sever disorder.

benzene cores because of the relatively long interplanar distance (4.6 \AA).¹⁵ The inclusion channels with undulated surfaces, run along the *c* axis, which is orthogonal to the RhomNet plane (Fig. 2d). A ratio of solvent accessible volume is at 58%. In the voids, highly-disordered *o*DCB molecules are included with a molar ratio of 1 : 4 (**X-Ph** : *o*DCB), which was estimated on the basis of thermogravimetric (TG) analysis (See, Fig. S1 in ESI).

X-TTF crystallized in space group *P-1* to give **X-TTF-1** with a RhomNet framework as shown in Fig. 3. Twisted angle of the phenylene groups and the TTF core ranges $32.6\text{--}43.8^\circ$. A rhombic void has a dimension of $14.9 \text{ \AA} \times 27.0 \text{ \AA}$. RhomNet sheet of **X-TTF** are stacked in an inclined ABAB manner with an average interlayer distance of 3.5 \AA . The first and second RhomNet layers (colored in yellow and red, respectively, in Fig. 3c) are largely overlap due to π/π stacking interactions between the TTF cores in addition to those between the phenylene

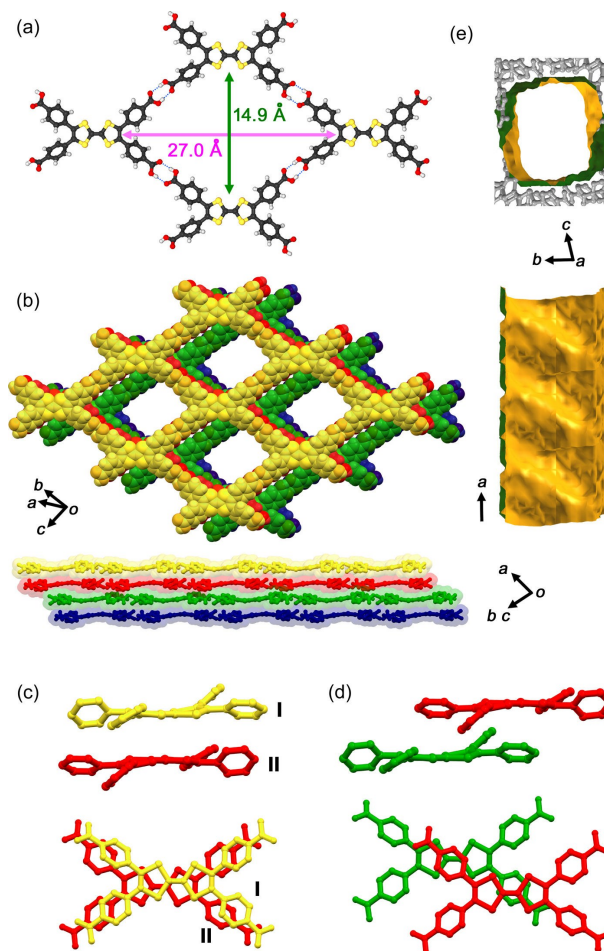


Fig. 3 Crystal structures of RhomNets **X-TTF-1** (a) hydrogen-bonded network motif composed of four molecules. (b) Selected four layers of porous rhombic sheets viewed from above (top) and side (bottom). (c) Orientation of two adjacent molecules, where the carboxyphenyl groups I and II are arranged in parallel manner. The carboxy groups are omitted for clarity in (c)-(left). (d) Visualized inclusion channel surface. Solvent molecules (i.e. *o*DCB) included in void spaces are omitted for clarity. Packing solvent molecules, see Fig. 4.

moieties: the interplanar distance between the stacked TTF cores is 3.4 \AA . The second and third layers (colored in red and green, respectively, in Fig. 3d), on the other hand are more slipped and show less overlap between TTF moieties. The inclusion channels run along the *a* axis and a ratio of solvent accessible volume is at 55% (Fig. 3e). Compared with **X-Ph-1**, the channel has a smooth surface. In the voids, *o*DCB molecules are included with a molar ratio of 1 : 4 (**X-TTF** : *o*DCB). Interestingly, only in this system, structures of four *o*DCB molecules are fully solved and refined

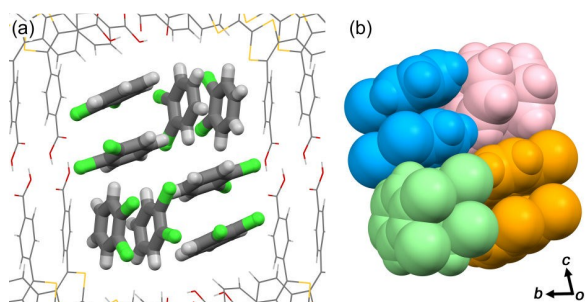


Fig. 4 Guest molecules (oDCB) packed with a sandwich-herringbone fashion in 1D channel of X-TTF-1 crystal. (a) Stick model, (b) Space-filling model.

crystallographically, probably due to specific conformity of the channel and guest molecules in size, shape and periodicity. As shown in Fig. 4, oDCB molecules form a face-to-face stacked dimer, and the dimers are packed with face-to-edge contacts, resulting a sandwich herringbone packing.¹⁶

Crystal X-PyQ-1, with space group *P*-1, consists of X-PyQ molecule with an inversion center. As same as the former systems, a hydrogen-bonded RhomNet framework is achieved even X-PyQ molecules possesses relatively basic pyrazine moieties (Fig. 5a). A rhombic void has a dimension of 12.5 Å × 28.7 Å. Twisted angle of the phenylene groups and the

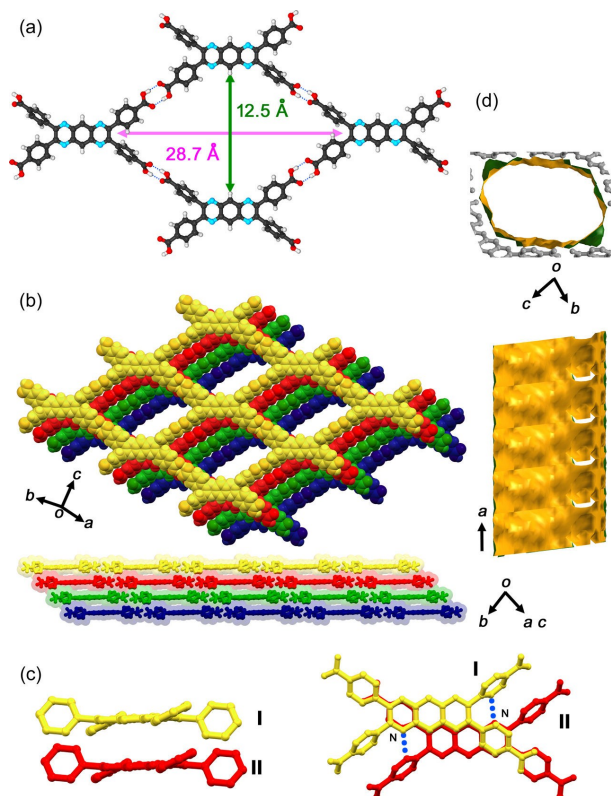


Fig. 5 Crystal structures of RhomNets X-PyQ-1 (a) hydrogen-bonded network motif composed of four molecules. (b) Selected four layers of porous rhombic sheets viewed from above (top) and side (bottom). (c) Orientation of two adjacent molecules, where the carboxyphenyl groups I and II are arranged in parallel manner. The carboxy groups are omitted for clarity in (c)-(left). (d) Visualized inclusion channel surface. Solvent molecules (*i.e.* oDCB) are included in void spaces, although those are not shown in Figures due to sever disorder.

pyrazinoquinoxaline core ranges 23.8–61.8°. RhomNet sheets of X-PyQ are stacked in an inclined AA manner with an averaged interlayer distance of 3.6 Å (Fig. 5b). Main interlayer interactions are π/π interactions between the pyrazine and peripheral phenylene moieties and CH/N interactions between the nitrogen atom in the core and the aromatic hydrogen atom (Fig. 5c). The inclusion channels run along the *a* axis and a ratio of solvent accessible volume is at 57%. oDCB molecules accommodated in the channels are highly disordered and a molar ratio of X-PyQ : oDCB was estimated at 1 : 5 based on TG analysis (See Fig. S1 in ESI).

Comparison of packing manners of the RhomNet sheets.

In Table 1, selected structural parameters of the present three RhomNet crystals are summarized. In connection with a conformation of X-shaped molecules, X-Ph has a large twisted angle (ω) due to steric hindrance of the peripheral phenylene groups, and therefore, the interlayer distance (*d*) is 4.6 Å, while the ω value of X-TTF is suppressed due to tight stacking of TTF moieties and the distance is much shorter (*d* = 3.5 Å). X-Ph, X-TTF and X-PyQ also have different molecular symmetry (C_2 , C_1 and C_i , respectively) in solid state, although they have the same symmetry in solution and gas phases. Due to the different molecular symmetry as well as interlayer interactions, the RhomNet sheets of X-Ph, X-TTF and X-PyQ stack in different ways in spite of the same network topology in the RhomNet sheets.

Table 1. Selected parameters of the RhomNet crystals.

	X-Ph-1	X-TTF-1	X-PyQ-1
space group	<i>Pbcn</i>	<i>P</i> -1	<i>P</i> -1
ω^a [°]	51.1–52.7 (51.9)	35.1–43.8 (36.6)	23.8–61.8 (42.8)
<i>d</i> ^b [Å]	4.56	3.53	3.55
(<i>h k l</i>) plane for RhomNet	0 0 1	1 -1 -1	1 3 3
molecular symmetry	C_2	C_1	C_i
Dimension of Rhombic motif	12.5 Å x 24.8 Å	14.9 Å x 27.0 Å	12.5 Å x 28.7 Å
Stacking manner	serrated	inclined	inclined
H:G ratio ^c	1 : 4	1 : 4	1 : 5
accessible volume ^d	58%	55%	57%

^aAveraged dihedral angle of carboxyphenyl groups against the central core.

^bAveraged interlayer distance. ^cMolar ratio of the X-shaped molecules and oDCB estimated based on TG analysis except for X-TTF-1, where the ratio was determined by crystallographic analysis. ^dCalculated by PLATON software.

Thermal analysis. To explore activation conditions of the channels, crystalline bulks of X-Ph-1, X-TTF-1, and X-PyQ-1 were subjected to thermogravimetric (TG) analysis, indicating that desolvation was completed at 200–250 °C (See, Fig. S1 in ESI). Powder X-ray

diffraction (PXRD) patterns of the as-formed crystals were also recorded upon heating to monitor structural changes upon desolvation. In the cases of **X-Ph-1** and **X-TTF-1**, new several peaks appeared in PXRD patterns upon heating. However, their intensity was weak, indicating that the resultant desolvated materials have low crystallinity, and further structural investigation was not

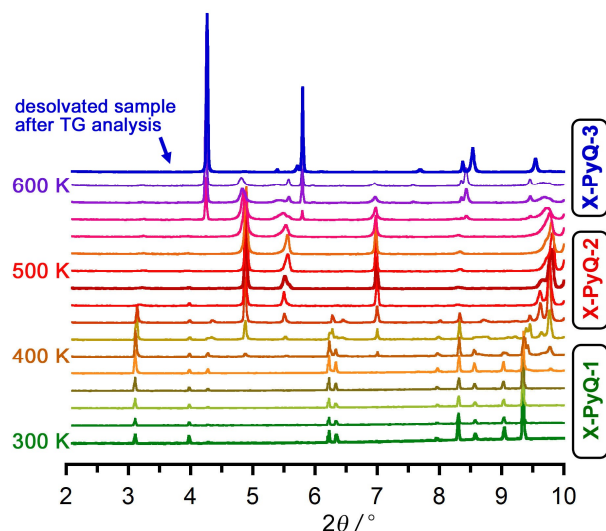


Fig. 6 PXRD pattern changes of X-PyQ upon heating from 300 K to 600 K stepped by 20 K. Pattern shown in top was recorded at room temperature after complete desolvation by heating. Wavelength of X-ray: 0.9997 Å.

performed. **X-PyQ-1**, on the other hand, show unambiguous changes and brought about intense peaks on a PXRD pattern upon heating, prompting us to investigate detailed structural changes. PXRD pattern changes of **X-PyQ-1** by heating up to 600 K are shown in Fig. 6. Peaks of as-formed crystalline bulk, for example at 3.1° and 4.0° ascribable to the 001 and 010 plane, respectively, disappeared below 500 K, while new peaks such as those at 4.9° and 5.6° appeared at ca. 400 K and became a dominant pattern at ca. 520 K, indicating formation of a new phase **X-PyQ-2**. Peaks attributed to **X-PyQ-2** subsequently decayed and replaced by another new phase with peaks at 4.2° and 5.8° at 600 K (**X-PyQ-3**). The pattern is in good agreement with a completely desolvated sample obtained after TG analysis (blue pattern in top of Fig. 6). These results indicate that crystal **X-PyQ-3** underwent thermal desolvation via intermediate state **X-PyQ-2** to give a completely desolvated apocrystal **X-PyQ-3**. The PXRD patterns indicate the unit cell parameters to be $a = 14.5 \text{ \AA}$, $b = 11.7 \text{ \AA}$, $c = 5.71 \text{ \AA}$, $\alpha = 89.7^\circ$, $\beta = 91.9^\circ$, $\gamma = 101.1^\circ$, *triclinic*, estimated space group: *P*-1, $V = 952.4 \text{ \AA}^3$ for **X-PyQ-2** and $a = 11.3 \text{ \AA}$, $b = 21.2 \text{ \AA}$, $c = 26.8 \text{ \AA}$, $\alpha = 90^\circ$, $\beta = 90^\circ$, $\gamma = 90^\circ$, *orthorhombic*, estimated space group: *Pbcm*, $V = 6467 \text{ \AA}^3$ for **X-PyQ-3**, respectively. Assuming that **X-PyQ-2** and **X-PyQ-3** contains one and eight molecules of **X-PyQ** within the cells, their crystal densities are 1.15 g/cm^3 and 1.36 g/cm^3 , respectively. The latter value is reasonable for common well-packed organic crystals, indicating no additional spaces within the cell. The former, on the other hand, seems to be smaller, indicating that the cell includes residual solvent molecules or empty spaces.

Conclusions

View Article Online

DOI: 10.1039/C7CE00183E

In conclusion, we demonstrated that three X-shaped tetracarboxylic acid derivatives with benzene, TTF, and pyrazinoquinoxaline cores (**X-Ph**, **X-TTF**, and **X-PyQ**, respectively) formed isostructural, hydrogen-bonded, rhombic network (RhomNet) sheets, which subsequently stacked without interpenetration to give low density frameworks with 1D inclusion channels (**X-Ph-1**, **X-TTF-1** and **X-PyQ-1**, respectively). This is the first demonstration that isostructural rhombic networks formed from a series of X-shaped tetracarboxylic acids with different π -conjugated cores through hydrogen bonds between carboxyl groups. It is remarkable that the RhomNet sheets of **X-Ph**, **X-TTF** and **X-PyQ** stack in different ways depending on conformation of the peripheral phenylene groups, molecular symmetry and interlayer interactions, in spite of the same network topology in the RhomNet sheets. The precise characterization of the present RhomNet crystals can provide a deeper structural insight of porous 2D-COFs.

Experimental

General.

^1H and ^{13}C NMR spectra were measured by a Bruker (600 MHz for ^1H , 150 MHz for ^{13}C) or JEOL (400 MHz for ^1H) spectrometer. Mass spectrum data were obtained from a JEOL JMS-700 instrument or autoflex III Bruker. Thermo gravimetric (TG) and differential thermal (DT) analyses were performed on Rigaku instruments ThermoPlusEvo2 8121 under an N_2 purge at a heating rate of $5 \text{ }^\circ\text{C min}^{-1}$.

Synthetic procedures

Pyrazinoquinoxaline derivative 3. Et_3N (0.5 mL) was added to a mixture of 1,2,4,5-tetraaminobenzene HCl salt (1.00 g, 3.53 mmol) in dry EtOH (100 mL). The reaction mixture was stirred for 3 min, and then dione **2** (2.35 g, 7.20 mmol) and acetic acid (1.0 mL) was added. The mixture was stirred for 20 h under reflux condition. After being cooled to room temperature, the precipitate was collected by filtration, washed with EtOH and dried in vacuo to give **3** (2.13 g, 2.96 mmol, 84%). M.p.: $360 \text{ }^\circ\text{C}$ (decomp.). ^1H NMR (600 MHz, CDCl_3): δ 9.09 (s, 2H), 8.07 (d, 8H, $J = 7.8 \text{ Hz}$), 7.69 (d, 8H, $J = 7.8 \text{ Hz}$), 3.91 (s, 12H) ppm. ^{13}C NMR (150 MHz, CDCl_3): δ 166.6, 154.4, 142.6, 140.6, 131.2, 130.1, 129.9, 129.6, 52.5 ppm. HR-MS (FAB): calcd. for $\text{C}_{38}\text{H}_{23}\text{N}_4\text{O}_8$ [$\text{M}+\text{H}$] $^+$ 663.1516; found: 663.1510.

X-PyQ. A suspension of **3** (0.706 g, 0.982 mmol) and KOH (0.368 g) in water (20 mL) and THF (100 mL) was stirred at $50 \text{ }^\circ\text{C}$ for 18 h. After removing THF in vacuo, 6 M-HCl aqueous solution was added dropwise to the reaction mixture till it becomes acidic. The resultant yellow precipitate was collected by centrifuge, washed with water and dried in vacuo to yield **X-PyQ** (0.541 g, 0.799 mmol, 79%) as dusty yellow solid. M.p.: $370 \text{ }^\circ\text{C}$ (decomp.). ^1H NMR (600 MHz, $\text{DMSO}-d_6$): δ 9.01 (s, 2H), 7.96 (d, 8H, $J = 8.4 \text{ Hz}$), 7.70 (d, 8H, $J = 8.4 \text{ Hz}$) ppm. ^{13}C NMR (150 MHz, $\text{DMSO}-d_6$): δ 166.9, 154.5, 142.2, 139.8, 131.4,

130.2, 129.1, 128.4 ppm. HR-MS (FAB): calcd. for $C_{42}H_{31}N_4O_8$ [M+H]⁺ 719.2142; found: 719.2136.

Single crystal X-ray measurement and analysis.

For crystals **X-Ph-1** and **X-PyQ-1**, diffraction data were collected on a two-dimensional X-ray detector (PILATUS 200K/R) equipped in Rigaku XtaLAB P200 diffractometer using multi-layer mirror monochromated Cu-K α radiation ($\lambda = 1.54187 \text{ \AA}$). The cell refinements were performed with a software CrysAlisPro.¹⁷ For crystals **X-TTF-1**, diffraction data were collected on a CCD (MX225HE, Rayonix) with the synchrotron radiation ($\lambda = 0.8000 \text{ \AA}$) monochromated by the fixed exit Si (111) double crystal. The cell refinements were performed with HKL2000 software.¹⁸ Direct methods (SHELXD,¹⁹ or SHELXT²⁰) were used for the structure solution of the crystals. All calculations were performed with the observed reflections [$I > 2\sigma(I)$] with the program CrystalStructure crystallographic software packages,²¹ except for refinement which was performed by SHELXL.²² All non-hydrogen atoms were refined with anisotropic displacement parameters, and hydrogen atoms were placed in idealized positions and refined as rigid atoms with the relative isotropic displacement parameters. SQUEEZE²³ function equipped in the PLATON program was used to remove disordered solvent molecules in the cavities for **X-Ph-1** and **X-PyQ-1**.

Table 2 Crystallographic data for **X-Ph-1**, **X-TTF-1** and **X-PyQ-1**

	X-Ph-1	X-TTF-1	X-PyQ-1
Empirical formula	$C_{34}H_{22}O_8$	$C_{34}H_{20}O_8S_4 \cdot 4(C_6H_4Cl_2)$	$C_{38}H_{22}N_4O_8$
Formula weight	558.54	1272.71	662.61
Crystal system	orthorhombic	triclinic	triclinic
Space group	<i>Pbcn</i>	<i>P-1</i>	<i>P-1</i>
<i>a</i> (Å)	19.4377(15)	10.0210(3)	5.60869(10)
<i>b</i> (Å)	30.6822(12)	16.1986(5)	14.7726(4)
<i>c</i> (Å)	9.1127(8)	18.3286(5)	18.7946(5)
α (°)	90	76.430(3)	75.237(2)
β (°)	90	87.497(2)	82.3657(18)
γ (°)	90	74.082(3)	88.5990(19)
<i>V</i> (Å ³)	5434.7(7)	2780.58(15)	1492.40(6)
<i>Z</i>	4	2	1
<i>T</i> (K)	253	93	113
<i>D_c</i> (g cm ⁻³)	0.683	1.524	0.737
Reflection collected	13201	17343	8334
Unique reflections	5384	9053	5985
Parameters	190	707	226
<i>R_{int}</i>	0.0629	0.0304	0.0339
GOF	1.360	1.034	1.107
<i>R₁</i> ^a [$I > 2\sigma(I)$]	0.1026	0.0540	0.0765
<i>wR₂</i> ^b (all data)	0.3439	0.1724	0.2723

Powder X-ray diffraction measurement.

The powder samples were loaded in a Lindemann glass capillary with 0.5 mm outer diameter. The diffraction data

were collected on 1D detector MYTHEN (Detectors) with the synchrotron radiation ($\lambda = 0.9997 \text{ \AA}$) monochromated by the fixed exit Si (111) double crystal at BL02B2 in SPring-8 with approval of JASRI (proposal Nos. 2015B1130 and 2016A1264).

Estimation of cell parameters.

Calculation was performed by using the Reflex Plus software implemented in Material Studio ver 6.0.²⁴ The powder patterns of **X-PyQ-2** and **X-PyQ-3** were indexed by the X-cell.²⁵

Acknowledgements

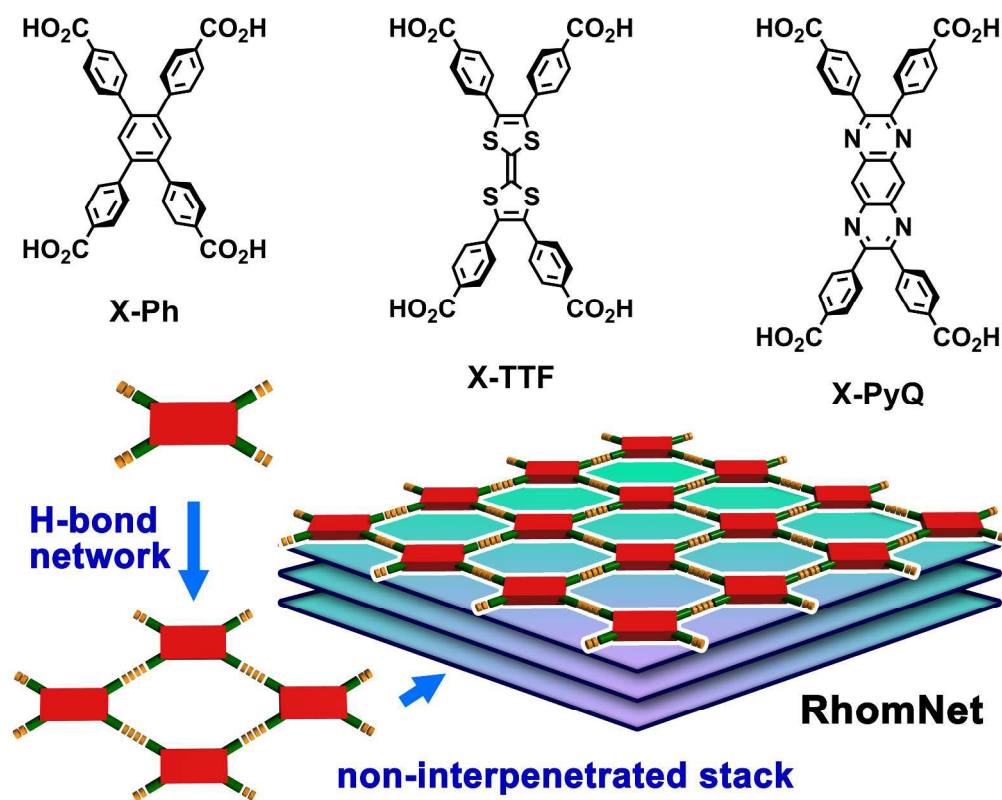
This work was supported by a Grant-in-Aid for Scientific Research (C) (JPT15K04591) and for Scientific Research on Innovative Areas: π -System Figuration (JP15H00998) from MEXT Japan. We would like to thank Prof. Hidehiro Sakurai, Osaka University, for NMR measurements and Prof. Hideki Yorimitsu, Kyoto University, for fruitful advice about derivatization of TTF. Crystallographic data were partly collected using synchrotron radiation at the BL38B1 and BL02B2 in the SPring-8 with approval of JASRI (Proposal Nos. 2015B1397, 2015B1130, 2016A1264).

Notes and references

- † CCDC numbers: **X-Ph-1** (CCDC-1499633), **X-TTF-1** (CCDC-1499634), **X-PyQ-1** and (CCDC-1499635) contain the supplementary crystallographic data for this paper. These data can be obtained free of charge from The Cambridge Crystallographic Data Centre via www.ccdc.cam.ac.uk/.
- 1 A. G. Skater and A. I. Cooper, *Science*, 2015, **348**, 988.
- 2 (a) X. Feng, X. Ding and D. Jiang, *Chem. Soc. Rev.* 2012, **41**, 6010. (b) S.-Y. Ding and W. Wang, *Chem. Soc. Rev.* 2013, **42**, 548; (c) N. Huang, P. Wang and D. Jiang, *Nat. Rev. Mater.* 2016, **1**, 16068.
- 3 For example, see; (a) M. Calik, F. Auras, L. M. Salonen, K. Bader, I. Grill, M. Handloser, D. D. Medina, M. Dogru, F. Löbermann, D. Trauner, A. Hartschuh and T. Bein, *J. Am. Chem. Soc.* 2014, **136**, 17802; (b) S. Chandra, T. Hundu, S. Kandamabath, R. BabaRao, Yogesh Marathe, S. M. Kunjir and R. Banerjee, *J. Am. Chem. Soc.* 2014, **136**, 6570; (c) S.-Y. Ding, M. Dong, Y.-W. Wang, Y.-T. Chen, H.-Z. Wang, C.-Y. Su and W. Wang, *J. Am. Chem. Soc.* 2016, **138**, 3031; (d) S. Chandra, D. R. Chowdhury, M. Addicoat, T. Heine, A. Paul and R. Banerjee, *Chem. Mater.* DOI: 10.1021/acs.chemmater.6b04178;
- 4 A. P. Côté, A. I. Benin, N. W. Ockwin, M. O'Keeffe, A. J. Matzger and O. M. Yaghi, *Science* 2005, **310**, 1166.
- 5 Q. Fang, Z. Zhongbin, S. Gu, R. B. Kaspar, J. Zheng, J. Wang, S. Qiu and Y. Yan, *Nat. Commun.* 2014, **5**, 4503.
- 6 B. Lukose, A. Kuc and T. Heine, *Chem. Eur. J.* 2011, **17**, 2388.
- 7 (a) L. Ascherl, T. Sick, J. T. Margraf, S. H. Lapidus, M. Calik, C. Hettstedt, K. Karaghiosoff, M. Döblinger, T. Clark, K. W. Chapman, F. Auras and T. Bein, *Nat. Chem.* 2016, **8**, 310; (b) F. Auras, L. Ascherl, A. H. Hakimioun, J. T. Margraf, F. C. Hanusch, S. Reuter, D. Bessinger, M. Döblinger, C. Hettstedt, K. Karaghiosoff, S. Herbert, P. Knochel, T. Clark and T. Bein, *J. Am. Chem. Soc.* 2016, **138**, 16703.
- 8 J. Lu and R. Cao, *Angew. Chem. Int. Ed.* 2016, **55**, 9474.
- 9 (a) Y. He, S. Xiang and B. Chen, *J. Am. Chem. Soc.* 2011, **133**, 14570; (b) W. Yang, A. Greenaway, X. Lin, R. Matsuda, A. J. Blake, C. Wilson, W. Lewis, P. Hubberstey, S. Kitagawa, N. R.

- Champness and M. Schröder, *J. Am. Chem. Soc.* 2010, **132**, 14457; (c) A. Yamamoto, T. Hirukawa, I. Hisaki, M. Miyata and N. Tohnai, *Tetrahedron Lett.* 2013, **54**, 1268.
- 10 (a) F. H. Herbstein, M. Kapon and G. M. Reisner, *J. Inclusion Phenom.* 1987, **5**, 211; (b) R. E. Melendez, C. V. K. Sharma, M. J. Zaworotko, C. Bauer and R. D. Rogers, *Angew. Chem., Int. Ed. Engl.* 1996, **35**, 2213; (c) A. R. A. Palmans, J. A. J. M. Vekemans, H. Kooijman, A. J. Spek and E. W. Meijer, *Chem. Commun.* 1997, 2247; (d) K. Kobayashi, T. Shirasaka, E. Horn and N. Furukawa, *Tetrahedron Lett.* 2000, **41**, 89; (e) K. Kobayashi, A. Sato, S. Sakamoto and K. Yamaguchi, *J. Am. Chem. Soc.* 2003, **125**, 3035; (f) D. Maspoch, N. Domingo, D. Ruiz-Molina, K. Wurst, J. Tejada, C. Rovira and J. Veciana, *J. Am. Chem. Soc.* 2004, **126**, 730; (g) P. Sozzani, S. Bracco, A. Comotti, L. Ferretti, R. Simonutti, *Angw. Chem. Int. Ed.* 2005, **44**, 1816; (h) B. K. Saha, R. K. R. Jetti, L. S. Reddy, S. Aitipamula and A. Nangia, *Cryst. Growth Des.* 2005, **5**, 887; (i) B. R. Bhogala and A. Nangia, *Cryst. Growth Des.* 2006, **6**, 32; (j) K. E. Maly, E. Gagnon, T. Maris, J. D. and Wuest, *J. Am. Chem. Soc.* 2007, **129**, 4306; (k) Y.-B. Men, J. Sun, Z.-T. Huang and Q.-Y. Zheng, *Angew. Chem. Int. Ed.* 2009, **48**, 2873; (l) X.-Z. Luo, X.-J. Jia, J.-H. Deng, J.-L. Zhong, H.-J. Liu, K.-J. Wang and D.-C. Zhong, *J. Am. Chem. Soc.* 2013, **135**, 11684; (m) T.-H. Chen, I. Popov, W. Kaveevivitchai, Y.-C. Chuang, Y.-S. Chen, O. Daugulis, A. J. Jacobson and O. Š. Miljanić, *Nature Commun.* 2014, **5**, 5131.
- 11 (a) I. Hisaki, S. Nakagawa, N. Tohnai and M. Miyata, *Angew. Chem. Int. Ed.* 2015, **54**, 3008; (b) I. Hisaki, N. Ikenaka, N. Tohnai and M. Miyata, *Chem. Commun.* 2016, **52**, 300; (c) I. Hisaki, S. Nakagawa, N. Ikenaka, Y. Imamura, M. Katouda, M. Tashiro, H. Tsuchida, T. Ogoshi, H. Sato, N. Tohnai and M. Miyata, *J. Am. Chem. Soc.* 2016, **138**, 6617; (d) I. Hisaki, S. Nakagawa, H. Sato and N. Tohnai, *Chem. Commun.* 2016, **52**, 9781.
- 12 For example, see: (a) O. K. Farha, K. L. Mulfort and J. T. Hupp, *Inorg. Chem.* 2008, **47**, 10223; (b) N. B. Shustova, B. D. McCarthy and M. Dincă, *J. Am. Chem. Soc.* 2011, **133**, 20126.
- 13 T.-Y. Zhou, S.-Q. Xu, Q. Wen, Z.-F. Pang and X. Zhao, *J. Am. Chem. Soc.* 2014, **136**, 15885.
- 14 (a) Y. Mitamura, H. Yorimitsu, K. Oshima, A. Osuka, *Chem. Sic.* 2011, **2**, 2017; (b) T. C. Narayan, T. Miyakai, S. Seki, M. Dincă, *J. Am. Chem. Soc.* 2012, **134**, 12932.
- 15 Interaction between aromatic rings. See: (a) S. Tsuzuki, K. Honda, T. Uchimarui, M. Mikami, K. Tanabe, *J. Am. Chem. Soc.* 2002, **124**, 104; (b) E. C. Lee, D. Kim, P. Jurečka, P. Tarakeshwar, P. Hobza, K. S. Kim, *J. Phys. Chem. A* 2007, **111**, 3446; (c) D. B. Ninković, G. V. Janjić, D. Ž. Veljković, D. N. Sredojević, S. D. Zarić, *ChemPhysChem* 2011, **12**, 3511.
- 16 G. R. Desiraju and A. Gavezzotti, *Acta Crystallogr. B* 1989, **45**, 473.
- 17 Rigaku Oxford Diffraction (2015), Software CrysAlisPro 1.171.38.410. Rigaku Corporation, Tokyo, Japan.
- 18 HKL2000. Z. Otwinowski and W. Minor, *Methods Enzymol.* 1997, **276**, 307.
- 19 G. M. Sheldrick, *Acta Crystallogr. Sect. A* 2008, **64**, 112.
- 20 G. M. Sheldrick, *Acta Crystallogr. A* 2015, **71**, 3.
- 21 Rigaku (2015). CrystalStructure. Ver. 4.2. Rigaku Corporation, Tokyo, Japan.
- 22 G. M. Sheldrick, *Acta Crystallogr. Sect. C* 2015, **71**, 3.
- 23 (a) P. v. d. Sluis and A. L. Spek, *Acta Crystallogr. Sect. A* 1990, **46**, 194-201. (b) A. L. Spek, *Acta Crystallogr. Sect. D* 2009, **65**, 148-155.
- 24 Material Studio ver 6.0; Accelrys Software Inc.: San Diego, CA, 2011.
- 25 M. A. Neumann, *J. Appl. Cryst.* 2003, **36**, 356.

View Article Online
DOI: 10.1039/C7CE00183E



960x780mm (100 x 100 DPI)